

A POWER MANAGEMENT SYSTEM FOR INTERCONNECTED AC ISLANDED MICROGRIDS USING BACK-TO-BACK CONVERTER

Ezenwa Udoha^{1}, Saptarshi Das², Mohammad Abusara³*

^{1,2,3}Faculty of Environment, Science and Economy, University of Exeter, Penryn Campus, United Kingdom.

**eu217@exeter.ac.uk Tel: +44(0)7767353468*

Keywords: POWER MANAGEMENT, INTERCONNECTED MICROGRID, RENEWABLE ENERGY SOURCES, GLOBAL DROOP CONTROL, BACK-TO-BACK CONVERTERS.

Abstract

Islanded AC microgrids are mini-power grids formed by assembling distributed generation sources, energy storage systems and loads. They are reliable and can operate at different voltages and frequencies to meet the requirements of the load. Interconnected Islanded Microgrids consist of multiple islanded microgrids interconnected to improve power system availability and stability, control flexibility, resiliency and reserve capacity. Islanded microgrids can be interconnected using back-to-back power converters to decouple connecting frequencies whose active and reactive power control can be done wirelessly and autonomously under a low communication link. This paper proposes a novel structure and control strategy using back-to-back converters and power transformers to interconnect multiple islanded AC microgrids to a global AC bus. Microgrids and global bus can utilise their resources to improve their operation and benefits. The control strategy uses a frequency signalling mechanism to limit the power demand of individual global converters and adjusts its droop coefficients accordingly and in proportion to deviation in frequency. The global droop controllers of the global connecting converters receive information about the status of the frequencies of individual microgrids using a low bandwidth communication link to enhance network power flow. MATLAB/Simulink results validate the performance of the proposed structure and control strategy.

1. Introduction

As the global demand for clean, efficient, and sustainable energy sources grows, microgrids have emerged as a promising solution to address these needs. Microgrids are local power networks that can operate independently and with the main power grid. The stiff power grid forms the microgrid bus frequency and voltage in grid mode. Also, the grid balances any difference between the power generated by the RES and that consumed by the load. The battery energy storage system (BESS) role controls the amount of power exchanged between the microgrid and the grid. In islanded mode, the BESS is the grid-forming unit that controls and maintains the AC bus voltage and frequency. The BESS balance the difference between the power generated by the RES and that consumed by the load. However, overcharging and undercharging boundaries are set to preserve the reserve capacity of BESS. The surplus power from RES can be curtailed to prevent overcharging of the BESS, while the auxiliary unit in the form of a diesel generator/micro gas turbine can be used to supplement power or eventual load shed. The rates of charging/discharging of BESS affect their rated capacity. Suppose the BESS is rapidly discharged; this lowers the battery capacity and reduces the amount of energy that can be extracted from the battery. However, more energy is extracted when the BESS are discharged at a prolonged rate, and the capacity is higher, thus dissipating greater energy. The BESS state of charge (SOC) is desired to be operated and maintained within the safest operable limit. Exceeding the SOC maximum charging/discharging operable limits can put the BESS at risk by reducing its lifespan. Effective coordination and control of

each microgrid SOC are vital in determining different operational modes to utilise more RES to provide better load support. Different literature on microgrids, [1]–[5] has achieved good control schemes for power management in individual microgrid units. However, system reliability and efficiency degrade as the load capacity and need for expansion increase. This is because more integration of RES in low voltage microgrid systems with high R/X line impedance ratio can lead to real and reactive power coupling and stability concerns[6][7]. Microgrids can accommodate a few RES, which can meet the minimal demand of loads. However, to overcome the above limitations and enhance flexibility, microgrids are interconnected to improve supply availability and provide better RES utilisation. Interconnected microgrids consist of two or more islanded microgrids connected to improve the average energy supply and reserve sharing capacity, operating in islanded (autonomous) and utility grid modes. Interconnected microgrids have a greater capacity to improve network reliability, flexibility, resiliency and sustainability[8]. Interconnected islanded microgrids can be operated at different voltages and frequencies to suit their load characteristics [9], [10]. The frequency and voltage of emerging networks can differ from other microgrids depending on load requirements [11]. Interconnected islanded AC microgrids have the potential to improve energy efficiency and reliability. That depends on whether adequate management is in place to boost the distinct benefits of the networks. The two main ways to interconnect and manage islanded microgrids are; a) common AC bus and b) common

DC bus. Using a common AC bus will allow existing overhead lines, power systems auxiliaries and loads to be connected without additional investments in power systems infrastructure, as would have been the case for a common DC microgrid. However, using a common DC bus will require time-consuming and cost-intensive investments in high-voltage DC (HVDC) technology. This complex and sophisticated technology is non-existent in the developing world. It is easier to interconnect islanded microgrids with the same voltage and frequency with static switches or breakers and a good synchronisation algorithm than those with different voltages and frequencies, which provides more autonomy and flexibility to the connected load [8], [9], [11], [12]. Multiple microgrids have been interconnected in different structures and topologies using common AC and DC (for grid-connected and islanded modes of operation) in various literature for their prime benefits. Somewhat related literature on interconnected AC microgrids presented in [9], [13], [14] consists of two microgrids interconnected with a back-to-back (AC/DC/AC) converter, and one microgrid is connected to the grid power. A robust distributed control for interconnected microgrids was designed [15] to regulate the power flow among multiple microgrids in island mode. This paper has three microgrids interconnected directly via a common bidirectional VSC-HVDC link, each with its own distributed generation (DG) units (photovoltaics (PV), converter-based wind generator) and STATCOM/ESS. However, the desired power regulation was achieved by developing a robust distributed control scheme which monitors the mismatch in real power, reactive powers and deviation in frequency that causes the controllers to communicate to regulate power flow directly through VSC-HVDC to meet demand. An optimal control of the active power-sharing capacity of interconnected microgrids presented in [16] consists of two microgrids directly interconnected via a tie-line. In [17], the inter-tied AC/AC microgrids are structured with two microgrids interconnected via a single back-to-back AC/DC/AC converter located between the microgrids. One microgrid has a frequency of 50Hz, and the other with a frequency of 60Hz. The latter is directly connected to a 60Hz utility grid. Power management in the multi-microgrid system proposed in [10] consists of a fixed utility grid connected to a voltage source converter (VSC), a circuit breaker, and an energy router with back-to-back converter technology (consisting of four VSCs with a common DC link) connected in parallel with four different microgrids (multi-microgrids). In [18], two community microgrids are interconnected via a shared DC bus. Each community microgrid consists of PV and Hybrid Energy Storage System (HESS); all are metered and connected to the DC-link through bidirectional DC-DC converters. A distributed optimal tie-line power flow control for multiple interconnected AC microgrids presented in [17] consists of multiple microgrids connected to the grid through a grid-tied switch. Two AC microgrids interconnected with a back-to-back converter in [19] exchanged active and reactive powers using local measurements of voltages and frequencies on the two sides of the BTBC. A power management strategy for interconnected microgrids proposed in [20] consists of three

microgrids structured to connect directly to each other via a tie-line, and each microgrid is made up of RES, a lithium battery and a diesel generator. A framework for a multi-microgrid to operate on different frequency qualities presented in [21] is interconnected with a common DC bus through an interlinking AC/DC converter. However, all the works on interconnected microgrids described in literature consist of related physical structures, interconnecting medium and controls such that the microgrids are either directly interconnected to one another via a tie-line or circuit breaker (in the form of a common AC bus) as seen in; [10][17] or single back-to-back converter (common DC bus) as seen in; [14][18][19][22] or HVDC-VSC converter located in-between two microgrids as proposed in [15]. However, none of the structures proposed in the literature provides a medium voltage bus with the common AC, adding extra flexibility, reserve capability, ease of expansion and stability to the interconnected microgrids as proposed in this research. Irrespective of widely publicised literature on the benefits of interconnected microgrids, this specific area of research remains untouched; no literature has sufficiently addressed microgrid interconnection with a robust common AC bus system.

This paper proposes a power management system for interconnected AC islanded microgrids using back-to-back converters and power transformers. The control strategy uses the frequency signalling mechanism to limit the power demand of individual global converters. It adjusts its droop coefficients accordingly and in proportion to deviation in frequency. The global droop controllers of the global DC/AC converters receive information about the status of the frequencies of individual microgrids using a low bandwidth communication link to enhance power flow among interconnected microgrids. The proposed system consists of three islanded AC microgrids, which explore the common AC (medium voltage AC (MVAC)) bus concept to provide a mechanism for interconnection using back-to-back converters and introduce traditional power transformers to boost the system's robustness. A back-to-back AC/DC/AC converter is an electrical mechanism to decouple the two connecting frequencies so that microgrids and the MVAC bus can autonomously utilise their distinct resources and benefits. Each islanded AC microgrid has a RES unit, BESS, auxiliary unit and loads. At the individual microgrid level, BESS is the grid-forming unit that regulates the voltage amplitude and frequency of the microgrid bus. The RES unit is the grid-feeding unit. The grid forming and grid feeding units are controlled to supply power to the AC bus or to supplement power from the auxiliary unit based on the requirements of the load using the conventional droop control strategy [3]. The local and global converters use a modified droop control strategy interconnected to regulate power flow in and out of the network. The main advantage of the global controller is that it uniformly and harmoniously regulates the voltage and the frequency of the global/MVAC bus collectively and wirelessly using a low-link communication network. It is important to state categorically that this research focuses on interconnected islanded AC microgrids, not grid connected.

Therefore, the novelty of this research can be highlighted in the structure and interconnection via back-to-back AC/DC/AC converter and power transformer to form a robust MVAC bus.

1.1. Novel Contribution to the Research

The following are novel contributions of the research:

- This research provides a novel structure and control topology by which interconnected microgrids can be developed for improved and robust power-sharing capacity and reliability. It also enhances flexibility by forming the MVAC bus, which transfers surplus power from distinct microgrid networks over long distances.
- Design of the controller that limits individual local converter power demand by monitoring the connecting converter DC-link voltage and adjusting the power demand to keep the DC-link voltage always controlled.
- Design of a novel controller that limits the power demand of individual global converters by measuring the frequency of each islanded AC microgrid and adjusting its droop coefficient accordingly and in proportion to the variation in the frequency. In addition, the controllers receive information about the frequencies of all local networks using a low bandwidth communication link to enhance power flow among interconnected microgrids. This strategy reduces the dependency on communication and the risk of instability in case of loss of communication links.

MATLAB/Simulink simulation results are presented to validate the performance of the proposed structure and control strategy. The remaining parts of the paper are arranged in the following format. Section II illustrates the system structure and control strategy, while Section III discusses the proposed control strategy for the local and global converter topology. Section IV presents the simulation results. Section V is the conclusion.

2. System Structure and Control Strategy

The structure of interconnected islanded AC microgrids considered in this paper is shown in Fig 1. The figure represents three islanded AC microgrids interconnected to the MVAC bus using back-to-back converters and traditional power transformers.

The structure consists of two distinctive converters, namely:

- DC/AC converters that connect the generation units to the respective microgrid bus, and
- Back-to-back AC/DC/AC converters connect the microgrids to the global (MVAC) bus.

The AC/DC/AC converter consists of the AC/DC local converter and DC/AC global converter (MVAC/global bus side). The local and global converters are linked together via a DC-link capacitor. The control strategy used for the generation units DC/AC converters is detailed in[3].

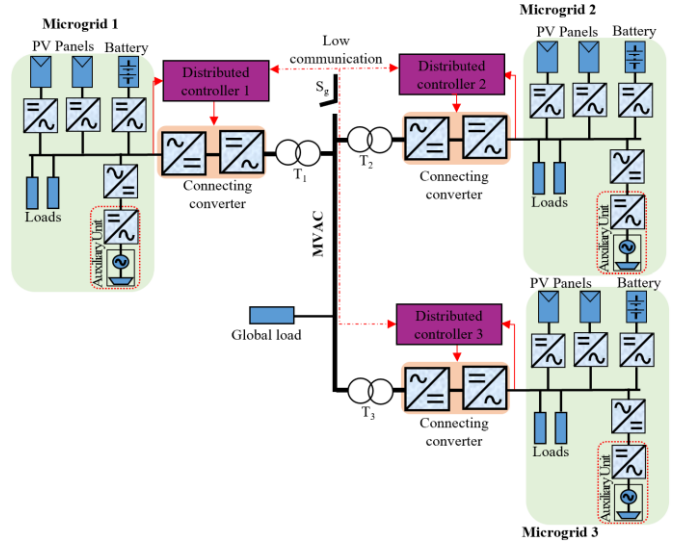


Fig. 1: Structure of Interconnected Islanded AC Microgrids.

- 1) The BESS is controlled to operate as the grid-forming unit, and the DC/AC inverter controls and maintains the AC bus voltage and frequency of each islanded microgrid. However, the microgrid frequency varies depending on the state of charge (SOC) of the BESS to send signals to other units.
- 2) The DC/AC converter of the PV-based RES unit is controlled to inject power into the microgrid bus. The DC/DC converter controls the PV output voltage to achieve maximum power point tracking (MPPT) and injects the maximum possible power given by solar unit. This can be realised by directly controlling the DC-link voltage with a PI controller and outer droop control.
- 3) The auxiliary unit in the form of a micro-gas turbine is interfaced by a unidirectional AC/DC converter equivalent to a passive rectifier and a DC/AC inverter. The AC/DC converter regulates the DC-link voltage while the DC/AC inverter controls the output power according to the AC bus frequency. The auxiliary unit supports the BESS unit to supplement power whenever the SOC is low, and the PV power cannot meet the load demand. It also imports power from other microgrids during a shortage, using the local frequency measurement to inject power.
- 4) The global converter (MVAC side converter) uses proportional droop control to determine power import and export. The droop coefficient is proportional, and the network frequency varies depending on the energy balance.
- 5) The local converter uses a PI controller to regulate and keep the DC-link voltage of the AC/DC converter always controlled.

At the interconnected microgrid level, the variations in the SOC reflect changes in the bus frequency. Power is exported if the frequency deviation is increased at a certain value above the nominal value. Similarly, power is imported if the frequency deviation is decreased at a certain value below the nominal. The amount of power exported or imported is proportional to the frequency deviations. However, any

substantial deviation in frequency in the microgrid brings about imbalance, and the global droop controller always responds to keep the system balanced. The DC/AC global converter control uses a global wireless droop control strategy to avoid the need for communication links between the units.

2.1. Droop Control Strategies for the Network Converters

This paper uses the wireless droop control strategy to mimic the behaviour of the synchronous generator in terms of decreasing the frequency when the active power is increased and vice versa[3]. The droop control principle is applied to all DC/AC inverters of all PV-based RES and BESS in all the microgrids, which have an output frequency ω , and voltage amplitude V , are given by the following mathematical expressions:

$$\omega = \omega_o^* - m_{p_i} (P - P^*) \quad (1)$$

$$V = V_o^* - n_{q_i} (Q - Q^*) \quad (2)$$

Where ω_o^* and V_o^* are the nominal frequency and nominal voltage references, m_{p_i} and n_{q_i} are the frequency proportional drooping coefficient and voltage proportional drooping coefficient, respectively. P , and Q are the measured active and reactive power while P^* and Q^* are active and reactive power setpoints, respectively.

3. Control for the Local and Global Converters

i). Local AC/DC Converter Control: The power demand of the local converter is controlled by the proportional and integral control described in the equation (3), which tends to keep the DC-link voltage always controlled by injecting more or less power into and out of the microgrid. The expression (3) gives the proposed power demand P_{local}^* for the local converter.

$$P_{local}^* = \left(k_{p_dc} + \frac{k_{i_dc}}{s} \right) (V_{dc} - V_{dc}^*) \quad (3)$$

Where V_{dc} and V_{dc}^* are the DC-link voltage and voltage setpoints, K_{p_dc} and K_{i_dc} are the proportional and integral controller values and 's' is the Laplace operator. This local converter droop controller measures the DC-link voltage and compares it with the reference signals, which represent the average voltage at the ABC terminal of the averaged model are connected to three phase series RL branch, which means the output impedance of the AC/DC converter which is interconnected to the microgrid.

ii). Global DC/AC Converter Control: The power demand of the global converter is controlled by controlling the frequency of the individual microgrid. The expression for the power demand P_{global}^* of the global converter is shown in the equation (4).

$$P_{global}^* = P(f_n - f_{MG}) \quad (4)$$

Where f_n and f_{MG} are the nominal and individual microgrid frequencies, and P is the proportional controller. This controller uses each microgrid AC bus frequency as a communication link, and the output of this controller sets the global converter's power demand. Figure 2 displays the control diagram for the local and global converter.

The frequency is at a nominal value during the normal operation of the interconnected microgrid. At this level, the different microgrids are operating within their desired load. Suppose the frequency of one microgrid goes up, indicating a surplus in power for that microgrid; the controller exports power from the microgrid to always keep the load balanced. At low-frequency deviation below nominal, indicating a shortage in power, the controller operates to supplement the power shortage to keep the system balanced. However, the greater the frequency deviation, the higher the power exported or imported to/from the microgrid.

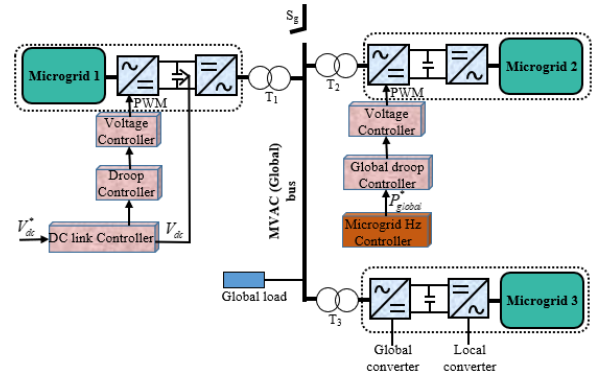


Fig. 2: Control Structure of the Local and Global Converter

Table 1. System Parameters

Parameter	Symbol	Value
Nominal bus frequency	$\omega_0 = 2\pi f_0$	314 rad/s
Nominal bus voltage	V_0	230V
Nominal DC-link voltage	V_{dc}	750V
DC link voltage P-controller gain	k_{p_dc}	20
DC voltage I-controller gain	k_{i_dc}	60
DC link capacitor	C_{dc}	1200 μ F
Active power droop coefficient	m	0.9e-4 rad/s/W
Reactive power droop coefficient	n	0.9e-4 V/Var
Frequency gain	k	30000

4. Simulation Results

The system consists of three islanded AC microgrids interconnected to the global bus with their respective connecting converters, and the proposed controllers have been designed and built in MATLAB/Simulink SimPower System. The main system parameters used in the simulation are shown in Table 1. However, due to the complex nature of the systems involved and to hasten the simulation speed, each microgrid is modelled as a 3-phase ideal voltage source (a block) in Simulink with appropriate parameters chosen from literature as in[4]. Also, each 3-phase local and global converter with the L filter has been modelled as an average model ideal converter. This averaged model is also a block provided in Simulink. The instantaneous active power used by the droop control equation is measured as a product of 3-phase individual voltages and currents of the different converters, together with a low pass filter, and this is represented as a block model in Simulink.

The simulation results are described in two cases. In each simulation scenario, the output of the DC link voltage controller sets the local converter's power demand, and the microgrid frequency controller's output sets the global converter's power demand.

- A) When the interconnected islanded AC microgrid operates with the power-sharing capability to complement each other in the network, the proportional controller determines the power demand of the global droop controller.
- B) When the interconnected network operates with no power-sharing capability, the proportional-integral controller is used to determine the power demand of the global droop.

Case A.1: Describes the simulation results when each of the three interconnected microgrids operates at a load of 40kw and a nominal frequency of 50Hz. Fig. 3 shows the power output and demand of the three microgrids, the connecting converters, the DC link voltages, and the frequencies. Fig. 3(a) - (d) shows that at the nominal operating frequency of 50Hz, represented in Fig. 3(d), all three microgrids operate to meet the demand of their respective loads at 40kw, and there is no power exchange. Each of the microgrid's local converter (LC) and global converter (GC) output power remains at 0kw, which is an indication of no power (P) exchange. Fig. 3(e) shows that the DC link voltage is constantly controlled at 750V.

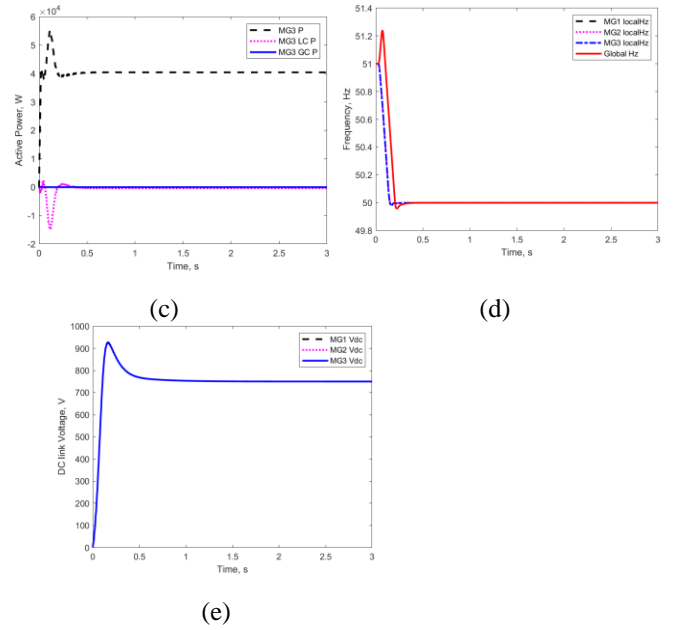
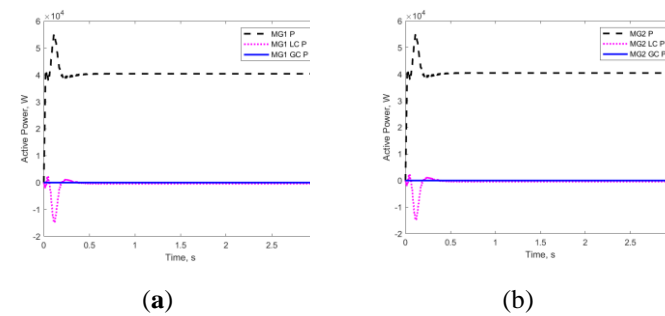
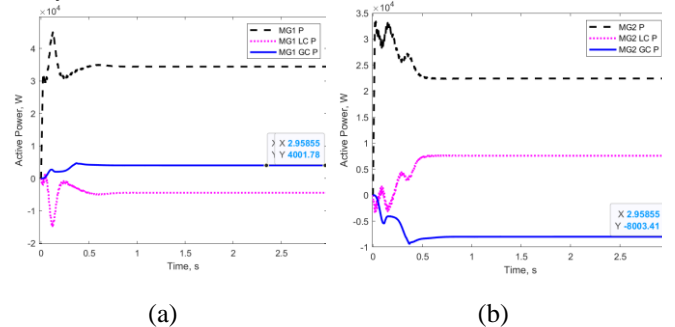


Fig.3: Output Responses when interconnected islanded microgrids are operated within the nominal frequency of 50Hz and 40kw load: (a) Output power and demand of microgrid one (b) Output power and demand of microgrid two (c) Output power and demand of microgrid three (d) Frequencies and (e) DC link voltages.

Case A.2: Describes the simulation results when each of microgrids one and three operate at a load of 30kw and nominal frequency of 50Hz, and microgrid two operates at a load of about 22kw, which reflects a deviation in frequency of 49.80Hz. Fig. 4 shows the power output and demand of three microgrids together with the connecting converters, frequencies and DC link voltages. Fig. 4(a) and Fig. 4(c) show that microgrid one and three operates to meet their different load demand of 30kw each and also exports their surplus power of about 4001.81w each equitably via their respective microgrid one and three global converters (MG1 GC and MG3 GC) to supplement the power deficiency in microgrid two. Fig 4(b) shows that microgrid two, with a deviation in frequency of 49.80Hz, as seen in Fig. 3(d), reflects a power shortage of 8003.46w. The microgrid two global converter (MG2 GC) indicates a power import from the global bus. Fig. 4(d) shows that microgrids one and two operates at nominal frequency of 50Hz, and the global bus frequency reset at 49.94Hz to keep the interconnected network balanced. Fig. 4(e) shows that the DC link voltage of microgrid one and two settled to its steady state at about 1sec while that of microgrid two reached its steady state value of 750V at about 1.5 secs.



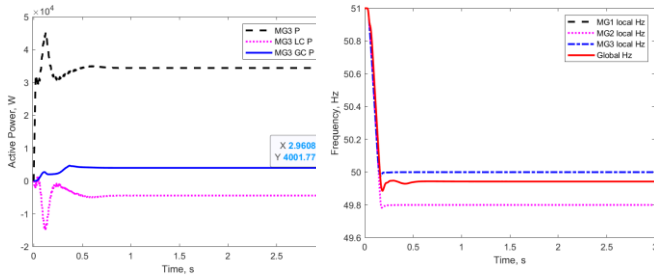


Fig.4: Output Responses when interconnected islanded microgrids one and three are operated within the nominal frequency of 50Hz and microgrid two at 49.80Hz: (a) Output power and demand of microgrid one (b) Output power and demand of microgrid two (c) Output power and demand of microgrid three (d) Frequencies and (e) DC link voltages

Case B: Illustrates the simulation results when the interconnected network operates with no power-sharing capability and the proportional controller is replaced with the proportional-integral controller. Each of the three interconnected microgrids operates at a load of 40kw and a nominal frequency of 50Hz, and microgrid two with power deficiency that reflects a deviation in frequency to 49.8Hz. Fig. 5 shows the power output and demand of the three microgrids together with the connecting converters, frequencies and DC link voltages. The simulation results of Fig. 5(a) – (c) show that there is no power export or import in the interconnected islanded microgrid network even at a deviation of frequency below nominal at 49.80Hz of microgrid two as shown in Fig. 5(d). Each microgrid operates independently to manage its loads; the global frequency remains at 50Hz. However, each microgrid's local converter (LC) and global converter (GC) output power remain at 0kw, indicating no power (P) exchange. Fig. 5(e) shows that the DC link voltage of the connecting converters reaches its steady state value of 750V at about 2.5secs.

Case B: Illustrates the simulation results when the interconnected network operates with no power-sharing capability and the proportional controller is replaced with the proportional-integral controller. Each of the three interconnected microgrids operates at a load of 40kw and a nominal frequency of 50Hz, and microgrid two with power deficiency that reflects a deviation in frequency to 49.8Hz. Fig. 5 shows the power output and demand of the three microgrids together with the connecting converters, frequencies and DC link voltages. The simulation results of Fig. 5(a) – (c) show that there is no power export or import in the interconnected islanded microgrid network even at a deviation of frequency below nominal at 49.80Hz of microgrid two as shown in Fig. 5(d). Each microgrid operates independently to manage its loads; the global frequency remains at 50Hz. However, each microgrid's local converter (LC) and global converter (GC) output power remain at 0kw, indicating no power (P) exchange. Fig. 5(e) shows that the DC link voltage of the connecting converters reaches its steady state value of 750V at about 2.5secs.

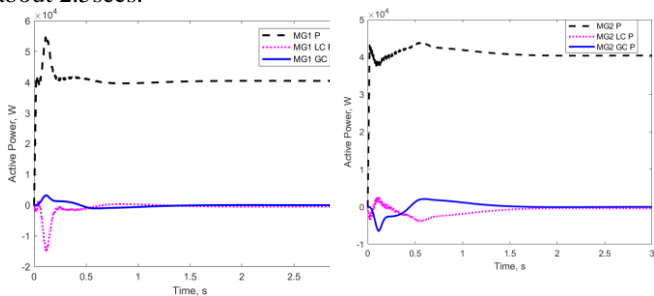


Fig.5: Output Responses when proportional controller is replaced with proportional-integral controller and microgrids one and three are operated within nominal frequency of 50Hz and microgrid two at 49.80Hz: (a) Output power and demand of microgrid one (b) Output power and demand of microgrid two (c) Output power and demand of microgrid three (d) Frequencies and (e) DC link voltages

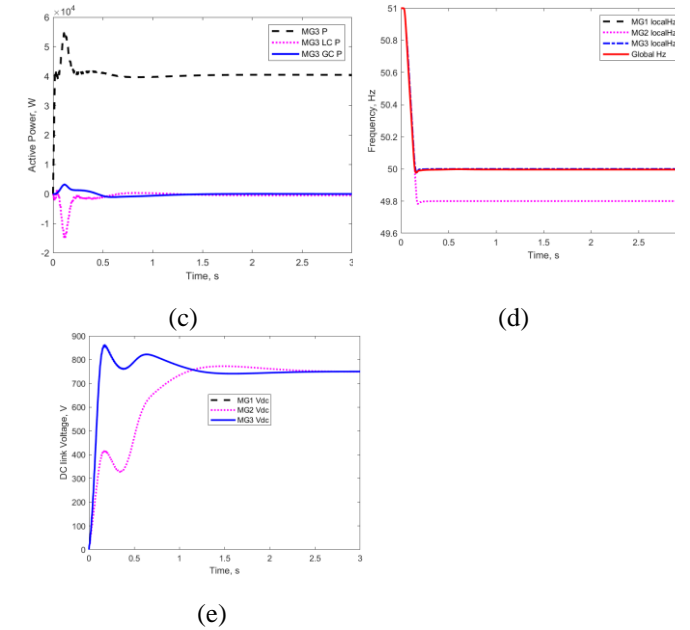


Fig.5: Output Responses when proportional controller is replaced with proportional-integral controller and microgrids one and three are operated within nominal frequency of 50Hz and microgrid two at 49.80Hz: (a) Output power and demand of microgrid one (b) Output power and demand of microgrid two (c) Output power and demand of microgrid three (d) Frequencies and (e) DC link voltages

5. Conclusion

In conclusion, a new structure and global droop control strategy based on frequency signalling technique have been proposed for power management of interconnected AC islanded microgrids using back-to-back converters. The interconnected microgrid structure uses traditional power transformers to form a robust common AC bus (global or medium AC (MVAC) bus) which adds more flexibility to the network and can transmit power over long distances. The associated global controllers of the connecting converters ensure that power leaves the microgrid with a surplus in power to the microgrid with a deficiency in power and vice versa to keep the interconnected network balanced. This is achieved by measuring the variation in AC bus frequency of the individual microgrids and ensuring that the local converters' DC link voltage is maintained within the limit. However, the controllers are implemented using local measurements without direct communication between the individual microgrid bus. Simulation results are presented to validate the performance of the network structure and controller operation.

6. Acknowledgements

This work is financially supported by the Nigeria Government Tertiary Education Trust Fund (TETFUND) through the Federal University of Petroleum Resources, Effurun (FUPRE) Academic Staff Training and Development (AST&D) 2018

intervention which provides a PhD grant for Ezenwa Udoha, grant number FUPRE/TO/AST&D/2018.

7. References

- [1] R. Al Badwawi, W Issa, T. K. Mallick, and M Abusara, ‘Power Management of AC Islanded Microgrids using Fuzzy Logic’, *IET Conference Publications*. 2016. doi: 10.1049/cp.2016.0348.
- [2] M. M. A. Abdelaziz, H. E. Farag, and E. F. El-Saadany, ‘Optimum droop parameter settings of islanded microgrids with renewable energy resources’, *IEEE Trans Sustain Energy*, vol. 5, no. 2, pp. 434–445, Apr. 2014, doi: 10.1109/TSTE.2013.2293201.
- [3] R. Al Badwawi, S. Member, W. R. Issa, T. K. Mallick, and M. Abusara, ‘Supervisory Control for Power Management of an Islanded AC Microgrid Using a Frequency Signalling-Based Fuzzy Logic Controller’, *IEEE Trans Sustain Energy*, vol. 10, no. 1, pp. 94–104, 2019.
- [4] W. R. Issa, M. A. Abusara, S. M. Sharkh, and A., ‘Control of Transient Power During Unintentional Islanding of Microgrids’, *IEEE Transactions on Power Electronics*, vol. 30, no. 8, pp. 4573–4584, 2015.
- [5] X. Yu, Z. Jiang, and Y. Zhang, ‘Control of parallel inverter-interfaced distributed energy resources’, *IEEE Energy 2030 Conference, Energy 2008*, doi: 10.1109/ENERGY.2008.4781030.
- [6] D. Rogers, A. M. Herscovitz, and K. Auth, ‘Power Africa: A U.S Government-led Partnership’, 2019. [Online]. Available: www.usaid.gov/powerafrica/nigeria
- [7] D. Idoniboyeobu and E. Udoha, ‘Impact of Distributed Generation in Power System Distribution Networks’, *IOSR Journal of Electrical and Electronics Engineering*, no. April, 2018, doi: 10.9790/1676-1302023247.
- [8] M. Naderi, Y. Khayat, Q. Shafiee, T. Dragicevic, H. Bevrani, and F. Blaabjerg, ‘Interconnected Autonomous ac Microgrids via Back-to-Back Converters — Part II: Stability Analysis’, *IEEE Transactions on Power Electronics*, vol. 35, no. 11, pp. 11801–11812, 2020.
- [9] I. U. Nutkani, P. C. Loh, and F. Blaabjerg, ‘Power flow control of interlinked hybrid microgrids’, *15th International Power Electronics and Motion Control Conference and Exposition, EPE-PEMC 2012 ECCE Europe*, no. 2, pp. 2–7, 2012, doi: 10.1109/EPEPEMC.2012.6397327.
- [10] M. Pham *et al.*, ‘Power management in multi-microgrid system based on energy routers’, *IEEE International Conference on Industrial Technology (ICIT) 2020*.
- [11] I. U. Nutkani, P. C. Loh, P. Wang, T. K. Jet, and F. Blaabjerg, ‘Intertied ac-ac microgrids with autonomous power import and export’, *International Journal of Electrical Power and Energy Systems*, vol. 65, pp. 385–393, 2015, doi: 10.1016/j.ijepes.2014.10.040.
- [12] M. Naderi, Y. Khayat, Q. Shafiee, T. Dragicevic, H. Bevrani, and F. Blaabjerg, ‘Interconnected Autonomous AC Microgrids via Back-to-Back Converters — Part I: Small-Signal Modeling’, *IEEE Transactions on Power Electronics*, vol. 35, no. 5, pp. 4728–4740, 2020.
- [13] I. U. Nutkani, P. C. Loh, and F. Blaabjerg, ‘Power flow control of intertied ac microgrids’, *IET Power Electronics*, vol. 6, no. 7, pp. 1329–1338, 2013, doi: 10.1049/iet-pel.2012.0640.
- [14] I. U. Nutkani, P. Chiang Loh, and F. Blaabjerg, ‘Distributed Operation of Interlinked AC Microgrids with Dynamic Active and Reactive Power Tuning’, *IEEE Transactions on Industry Applications*, vol. 49, no. 5, pp. 2188–2196, 2013. doi: 10.1109/TIA.2013.2262092.
- [15] J. Hossain *et al.*, ‘Design of Robust Distributed Control for Interconnected Microgrids’, *IEEE Transactions on Smart Grid*, vol. 7, no. 6, pp. 2724–2735, 2016.
- [16] D. H. Tungadio, ‘Optimal Control of Active Power Sharing Capacity of Microgrids Interconnected’, *Proceedings - 18th IEEE/ACIS International Conference on Computer and Information Science, ICIS*, pp. 67–71, 2019.
- [17] Y. Liu, Y. Li, H. Xin, H. B. Gooi, and J. Pan, ‘Distributed Optimal Tie-Line Power Flow Control for Multiple Interconnected AC Microgrids’, *IEEE Transactions on Power Systems*, vol. 34, no. 3, pp. 1869–1880, 2019.
- [18] D. Gamage, X. Zhang, A. Ukil, and A. Swain, ‘Energy Management of Islanded Interconnected Dual Community Microgrids’, in *IECON 2020 The 46th Annual Conference of the IEEE Industrial Electronics Society*, 2020, pp. 1803–1807. doi: 10.1109/IECON43393.2020.9254619.
- [19] M. Naderi, Y. Khayat, Q. Shafiee, and T. Dragicevic, ‘An Emergency Active and Reactive Power Exchange Solution for Interconnected Microgrids’, *IEEE Journal of Emerging and Selected Topics in Power Electronics*, vol. 9, no. 5, pp. 5206–5218, 2021. doi: 10.1109/JESTPE.2019.2954113.
- [20] Marwa GRAMI, M. REKIK, and L. KRICHEN, ‘A Power management Strategy for Interconnected Microgrids’, *20th International conference on Sciences and Techniques of Automatic Control & Computer Engineering (STA)*, 2020 pp. 213–218.
- [21] T. Nguyen, S. Member, H. Yoo, and S. Member, ‘A Droop Frequency Control for Maintaining Different Frequency Qualities in a Stand-Alone Multimicrogrid System’, *IEEE Trans Sustain Energy*, vol. 9, no. 2, pp. 599–609, 2018, doi: 10.1109/TSTE.2017.2749438.
- [22] B. Zhao *et al.*, ‘Energy Management of Multiple Microgrids Based on a System of Systems Architecture’, *IEEE Transactions on Power Systems*, vol. 33, no. 6, pp. 6410–6421, 2018.